SDC-93-428

SDC
SOLENOIDAL DETECTOR NOTES

DEADTIME OF SDC STRAW DETECTORS

January 1993

D. Craig, W.T. Ford and S.V. Greene
University of Colorado

SDC – 93 – 428
COLO – HEP – 307
January, 1993

Deadtime of SDC Straw Detectors

D. Craig, W. T. Ford, and S. V. Greene

Department of Physics, University of Colorado
Boulder, Colorado 80309-0390

The principle limitation on the efficiency of the SDC straw tube tracker will be pileup losses. We report here measurements and calculations to assess the expected deadtime.

The deadtime associated with each detected signal comes from two sources: (1) the TMC digitizer[1] records only one leading edge from its input stream in each clock-synchronized 32 ns interval; and (2) the output of the discriminator which drives the TMC remains high for the time its input stays above threshold. Relative to the initial particle crossing time, the leading edge of the gas-amplified ionization electron cluster charge arrives with nearly constant probability over a time interval equal to the maximum drift time in the straw, about 30 ns in a 2 T magnetic field; about 20 ns for $B = 0$. The last cluster arrives at the end of this interval.

The time dependence of the collected charge is given by[2,3]

$$q(t) = \frac{Q}{2\log\frac{b}{a}}\log(1+\frac{t}{t_0}),$$

where Q is the total charge liberated in the gas avalanche, and a and b are the anode and cathode radius, respectively. This expression applies to a short, unterminated detector; for the long modules a factor 1/2 is needed to account for the absorption in the terminating resistor of the charge which flows away from the readout connection.

The time parameter t_0 characterizes the positive ion drift:

$$t_0 = \frac{a^2\log(b/a)}{2\mu^+(V_0/p)}.$$

Here μ^+ is the positive ion mobility at 1 atm, V_0 is the chamber high voltage, and p is the pressure in atmospheres.

The function $q(t)$ exhibits a fairly rapid early rise that rolls off to a much slower approach to the limiting value Q. The amplifier-shaper-discriminator (ASD) circuit[4] is designed to detect these pulses with high sensitivity and minimal recovery time. The amplifier-shaper differentiates $q(t)$ with a 5-10 ns time constant, and a tail cancellation stage simulates the slow tail associated with the positive ion drift and subtracts this from the amplified pulse.

The width of the ASD output pulse as a function of the input charge has been simulated with SPICE.[5] With assumed detector capacitance of 10 pF, t_0 of 1.5 ns, ASD threshold of 1.75 fC, and effective integration time of 5 ns, the result plotted in Fig. 1 was found. (Fig. 1 also includes results of measurements which we discuss below.) The width increases with pulse charge, but rather slowly after reaching 20 ns or so.

To verify these results, we have measured pulse width distributions for both Fe^{55} and cosmic ray pulses in a prototype chamber. The chamber is one of

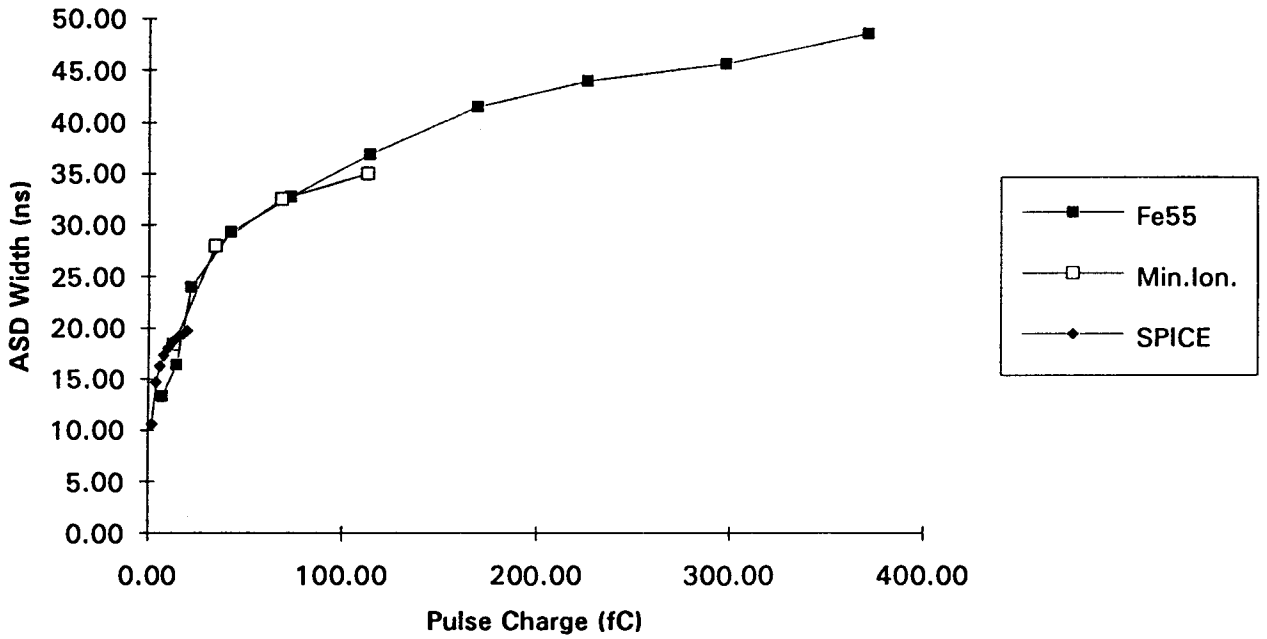

Fig. 1. Discriminator output width, predicted and observed, as a function of the input pulse charge.

the Indiana-built 12 inch, 64 cell units. The sense wire diameter is 25 μm, the cathode diameter is 4 mm, and there is no terminating resistor. The gas was $CF_4 - iC_4H_{10}(80/20)$. The atmospheric pressure at the elevation of our laboratory is about 0.83 atm.

The sense wires are connected through short micro coaxial cables to four 16-channel A-S-D8/T4 front end boards, operated at a charge threshold of about 3 fC. Pulse waveforms are shown in Fig. 2 for Fe^{55} signals viewed at the amplifier-shaper output and after tail cancellation. The Fe^{55} pulses are sharper, and larger at a given operating voltage, than minimum ionizing tracks because all of the X-ray energy is deposited very locally.

We have also recorded cosmic ray pulses by triggering the oscilloscope on a coincidence between two scintillation counters placed one above and one below the straw module. The scintillators measure about $1\frac{1}{4} \times 12$ inches and are separated by about 3 inches. This configuration accepts cosmic rays over a wide range of zenith angle, giving variations in track length within the straws. Typical discriminator output pulses are shown for these triggers in Fig. 3. A distribution of the observed widths taken at 1700 volts is shown in Fig. 4. The mean of the distribution is 32 ns.

We are interested in the deadtime as a function of pulse amplitude because a wide variation will occur in the detectors in the SDC configuration. This is because of both attenuation (the straws are up to 4 m long and have an attenuation length of about 6.3 m[6]), and because the path length in a detector of fixed radial thickness varies with polar angle as the cosecant. Fig. 5 shows the calculated variation with rapidity.

To express the operating conditions of our measurements in terms of input pulse charge, we need to estimate a number of factors. Following discussions documented in various publications and collaboration notes[3,7,8] we use the following (see Appendix):

1. An X-ray from Fe^{55} deposits 6.0 keV (average of lines at 5.9 and 6.5 keV),

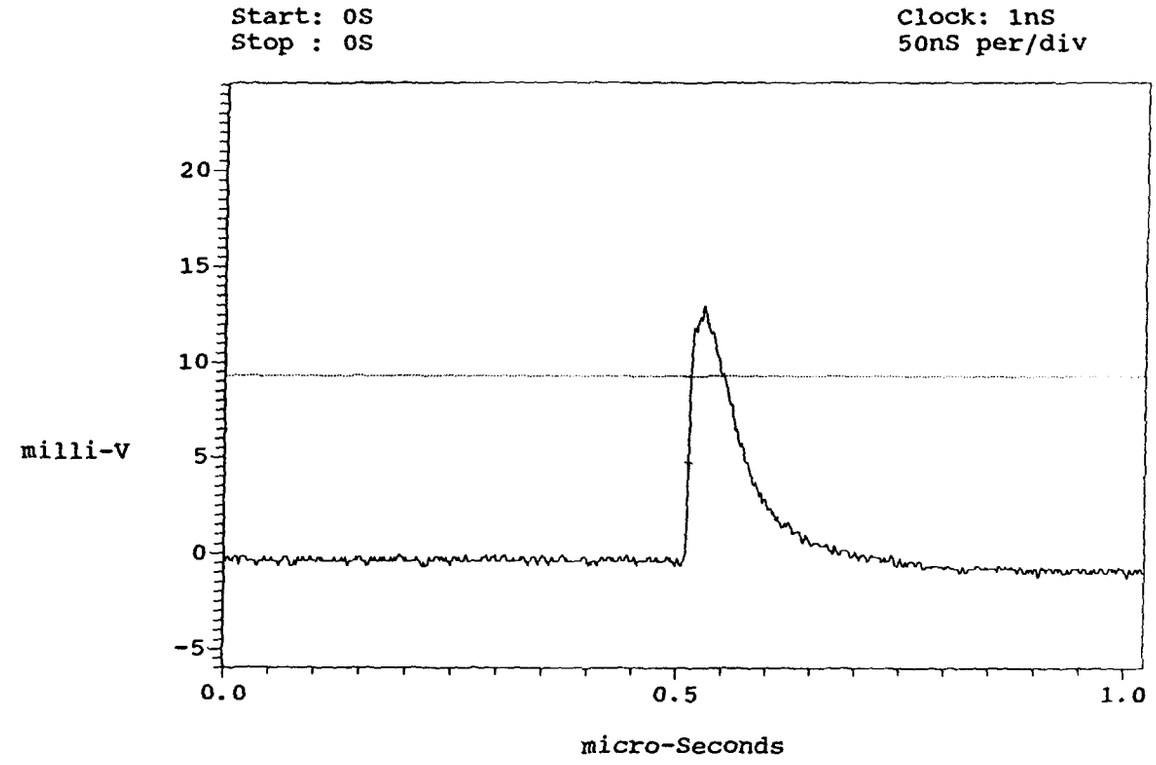

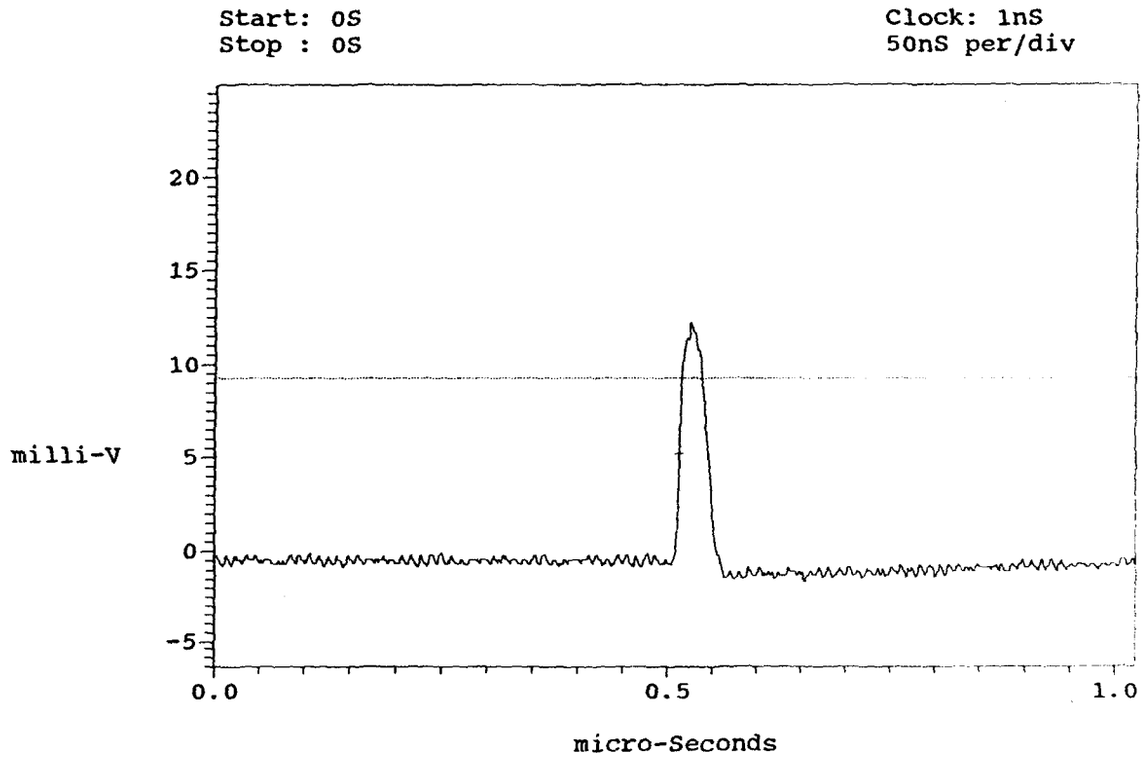

Fig. 2. Waveforms for Fe^{55} induced pulse in a prototype straw chamber. Amplifier-shaper output (above) before, and (below) after tail cancellation.

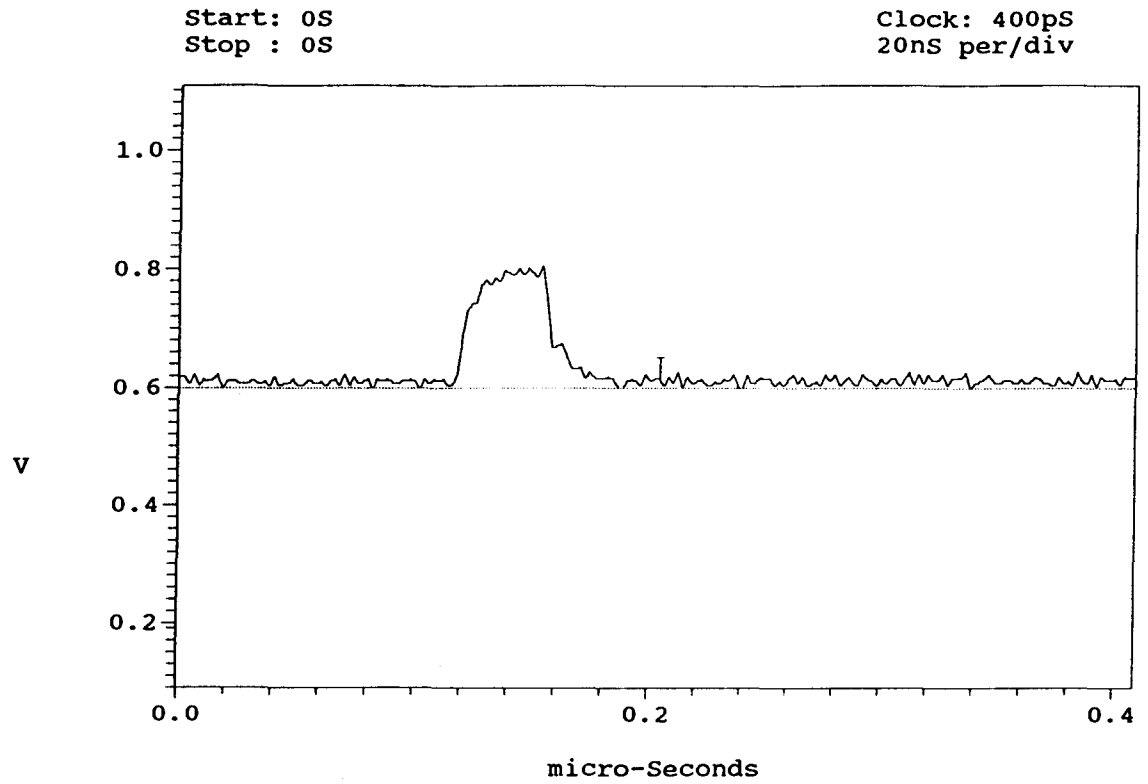

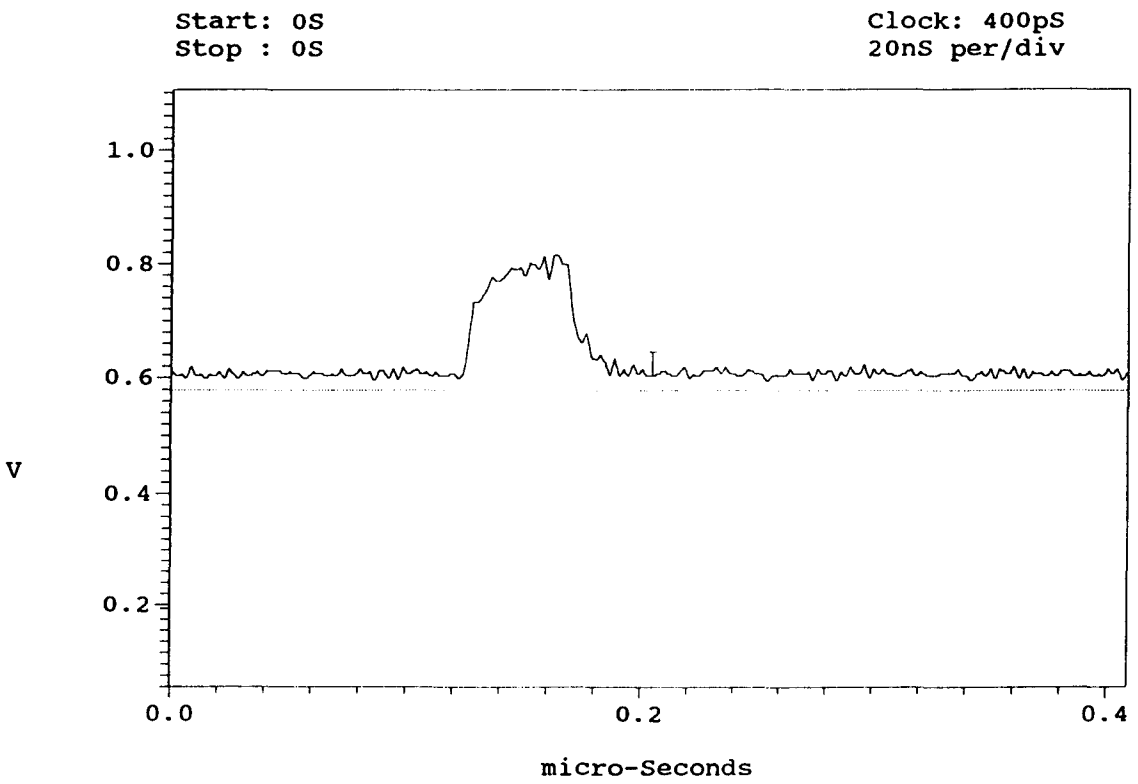

Fig. 3. Typical discriminator outputs for cosmic ray induced pulses.

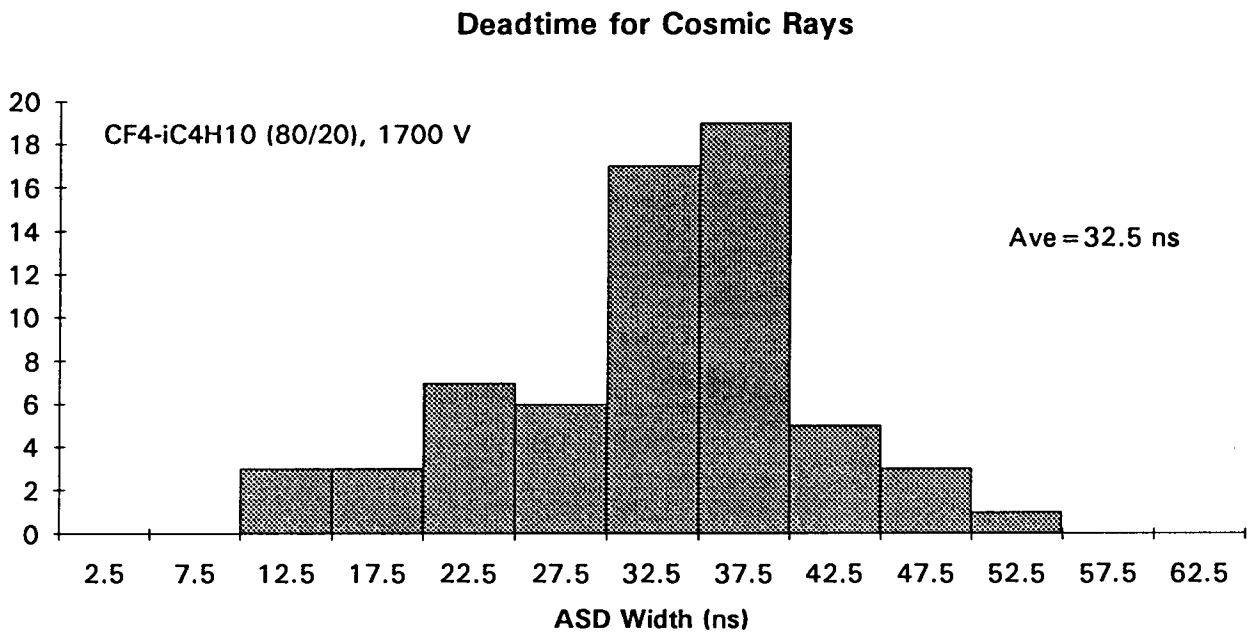

Fig. 4. Distribution of discriminator output widths observed for cosmic ray triggers for test chamber operated at 1700 V ($V/p = 2050$, gain $\simeq 5 \times 10^4$).

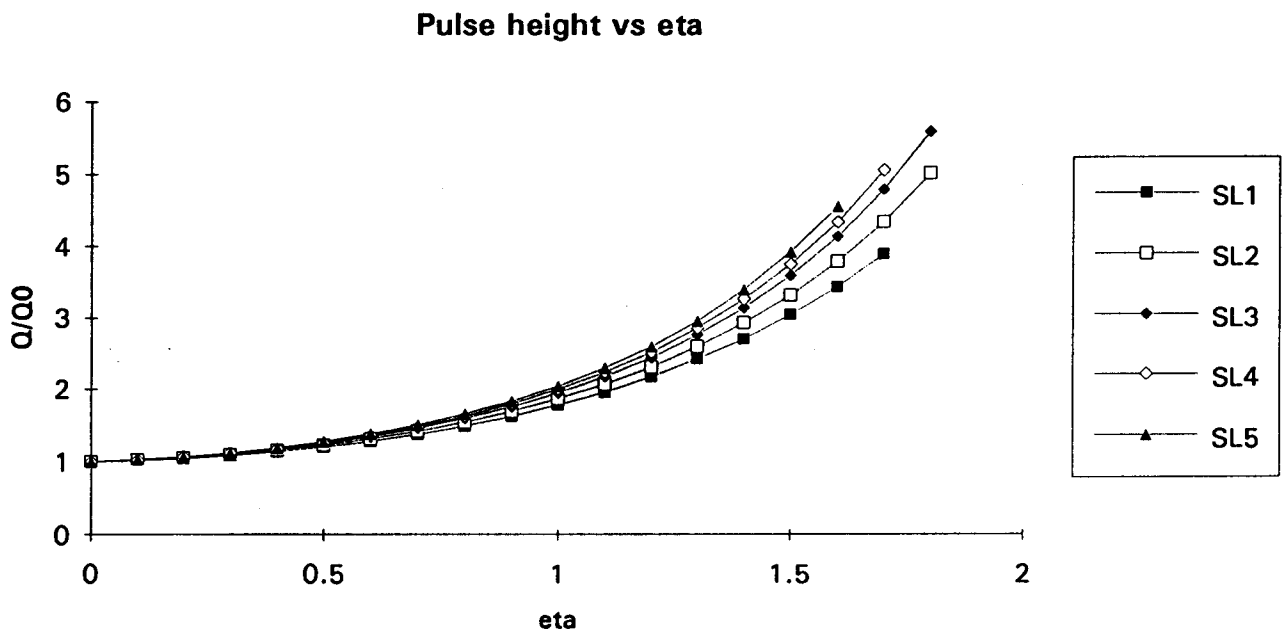

Fig. 5. Relative charge detected for charged tracks as a function of rapidity, allowing for path length within the cell and pulse attenuation.

generating a primary electron for each 34.3 eV on average.[9]

2. A minimum ionizing particle liberates $4.55 \sum Z_i$ electrons per cm at atmospheric pressure,[10] (Z_i is the atomic number of the ith atom in the molecule) or 153 electrons/cm for our gas mixture allowing for the reduced pressure, and $40p = 33.2$ clusters.[8] From these numbers we find that at the primary ionization site there are 3.8 electrons/cluster (independent of p).

3. We take the path length for cosmic rays to be the average chord length $= \frac{\pi}{4}$ times the 4 mm cell diameter, times the average secant of the zenith angle. We calculated the latter analytically from the scintillator geometry and the $\cos^2\theta$ distribution for cosmic rays, obtaining $\langle \sec\theta \rangle = 1.11$. For the ratio of Fe^{55} to minimum ionizing pulse heights we calculate 3.3 and measure 2.55 ± 0.15.

4. Because of electron attachment the number of electrons per cluster is reduced about a factor of two before the primaries reach the avalanche region. This affects Fe^{55} and minimum ionizing induced signals equally. We ignore any reduction in the attachment loss caused by the lower pressure, the uncertainty on the loss factor being larger.

5. We evaluate $q(t)$ from the formula given above, taking the ASD integration time t to be 8 ns, the value which reproduces the charge fraction found by convolution with a shaping function.[7] Neither attenuation nor the termination loss factor applies to our detector.

6. We take the gas gain at each voltage setting from the curve of Fig. 6, reproduced from Ref. 11, interpreting the abscissa as V/p. Here "Gain" is the effective gain, defined as charge generated in the avalanche per unit charge liberated by the primary ionization. Thus the effect of any losses by electron attachment is counted as a reduction of the effective gain. (In the appendix we refer to the efficiency for surviving attachment, E_{as}; the effective gain is $E_{as} \times G$, with G the avalanche gain.)

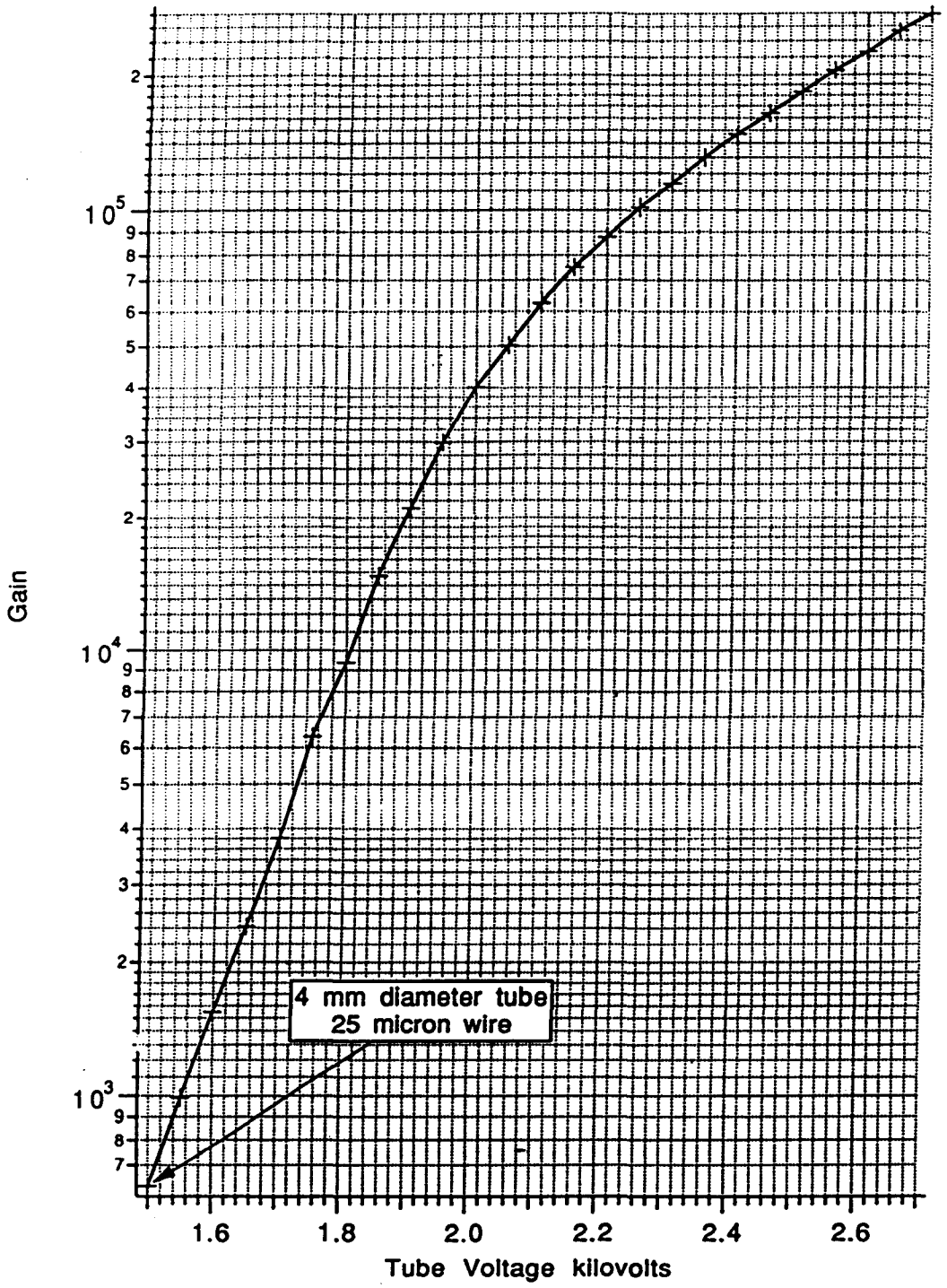

Fig. 6. Effective gain $E_{as} \times G$ vs high voltage for the prototype straw detector.

The resulting curves of pulse width vs charge are shown in Fig. 1. Statistical errors for the cosmic ray widths are about 5%, and the scale uncertainty in the abscissa from the charge normalization factors discussed above is about 30%. These effects, and differences in time constants, threshold settings, track length (for cosmic rays), primary pulse shape (for Fe^{55}), etc., between the SPICE simulation and the actual conditions of the measurement may or may not account for the lower level of the "flat" part of the curve for the simulation. However, the qualitative behavior is consistent for all three determinations, which confirm that the growth of pulse width with amplitude is well controlled over a wide range of amplitudes. For a scale relevant to the SDC configuration, we estimate that at a gain of 50,000 tracks near $\eta = 0$ produce about 20 fC at the ASD; Fig. 5 shows that the large η pulses will be about 5 times larger, or 100 fC. Even at three or four times this gain the large pulses remain less than 50 ns wide.

The drift velocity in the magnetic field will be about 70% of the zero field value, which would tend to widen all pulses a little compared with our measurements. As a rough guess we may add 10 ns in quadrature with the measured widths. We conclude that a conservative estimate of dead time, averaged over the axial length of the detectors, is about 40 ns. The 32 ns frame of the TMC digitizer circuit is well matched to the ASD output width and contributes very little to deadtime losses.

In the simulations we account approximately for deadtime effects by assuming a 40 ns constant, updating, time shadow for each hit. Digitizations falling within this interval of any previous hit (whether that previous hit made a digitization or not) are dropped from the digitization list. This should be an adequate representation of the effects of charged particles traversing the detector.

We do not address in this note possible anomalous responses of the electronics to very large pulses; these are the subject of other work in progress within the straw collaboration.

REFERENCES

1. Y. Arai, M. Ikeno and T. Matsumura, KEK Preprint 91-202 (subm. to IEEE, 1992).
2. F. Sauli, CERN 77-09 (1977).
3. H. Iwasaki, SDC Note SSC-SDE-8 (1989).
4. F. M. Newcomer et al., *Nuclear Instr. and Methods A* **283** (1989) 806.
5. M. Newcomer, private communication.
6. D. Rust, Procedings of May, 1992, SDC Meeting at KEK, SDC-92-276, p. 935.
7. H. Ogren, Straw Group Informational Memos 10 and 16 (1992).
8. J. Fischer, A. Hrisoho, V. Radeka, and P. Rehak, *Nucl. Instr. and Methods* **A238** (1985) 249-264.
9. G. F. Reinking, et al., *Journal of Appl. Physics* **60** (1986) 499.
10. J. Fehlman and G. Viertel, Compilation of Data for Drift Chamber Operation, ETH Zürich (1983).
11. SDC Straw Tracking Group, **Conceptual Design Report for the Modular Straw Outer Tracking System**, SDC Report SDC-91-00125 (1991).

Appendix

Electron and cluster yields for drift gases

Lehlman & Viertel: For min. ion., no. produced electrons, Nep = Nep0*SUMmolecule(Z).	Nep0	4.55 /cm				
Fischer, et al. find no. of produced clusters Ncp = Ncp0*SUMmolecule(Z).	Ncp0	1.19 /cm		Av. straw thickness = (pi/4)*4mm	0.31 cm	
For these gases:	Z	Nep/cm	Ncp/cm	Ned/straw (normal incidence)	Ncd/straw	RFe
CF4	42	191.10	50.00	30.24	13.42	2.91
iC4H10	34	154.70	40.48	24.48	10.86	3.60
CF4(80)+iC4H10(20)	40.4	183.82	48.10	29.09	12.91	3.03
Fe55		174.93	1.00	88.12	1.00	1.00

(For measurements in Boulder, apply a factor p/p0 = 0.83 and zenith factor to these numbers.)

Zenith angle factor	1.11					
	Z	Nep/cm	Ncp/cm	Ned/straw (zenith average)	Ncd/4mm	RFe
CF4	42	158.61	41.50	27.86	12.36	3.16
iC4H10	34	128.40	33.60	22.56	10.01	3.91
CF4(80)+iC4H10(20)	40.4	152.57	39.92	26.80	11.89	3.29
Fe55		174.93	1.00	88.12	1.00	1.00

Fischer, et al. measure Nc for CF4 = 41. Hypothesis: this is the number detected, and 41 vs 50 represents efficiency for detecting cluster after recombination (actually 50->48 by dilution).

If so, this efficiency = 1-EXP(-Necd), where Necd = no. of detected electrons/cluster.	Necd	1.93
Also, no. of produced electrons/cluster Necp = Nep0/Ncp0:	Necp	3.82
And the attachment survival efficiency Eas = Necd/Necp:	Eas	0.50
Fe55, X-ray av energy EFe = 6.0 keV	EFe	6000.00
Effective ion. potential IFe = 34.3 eV	IFe	34.30

Thus Ncp=1 and Necp=EFe/IFe

Detected charge/det. electron Qed (in fC*10^4) = (e/2/LN(b/a))*LN(1+t/t0), where b, a are cathode, wire radius, t0(ns)= 10^9a^2log(b/a)/(2muplusV/p). Divide by 2 for long, terminated detector.

e	1.60	a	1.25E-03	b	0.20	
t	8.00	muplus	1	Qed/e(1700V/.83)		0.16

Measured Gain includes Eas
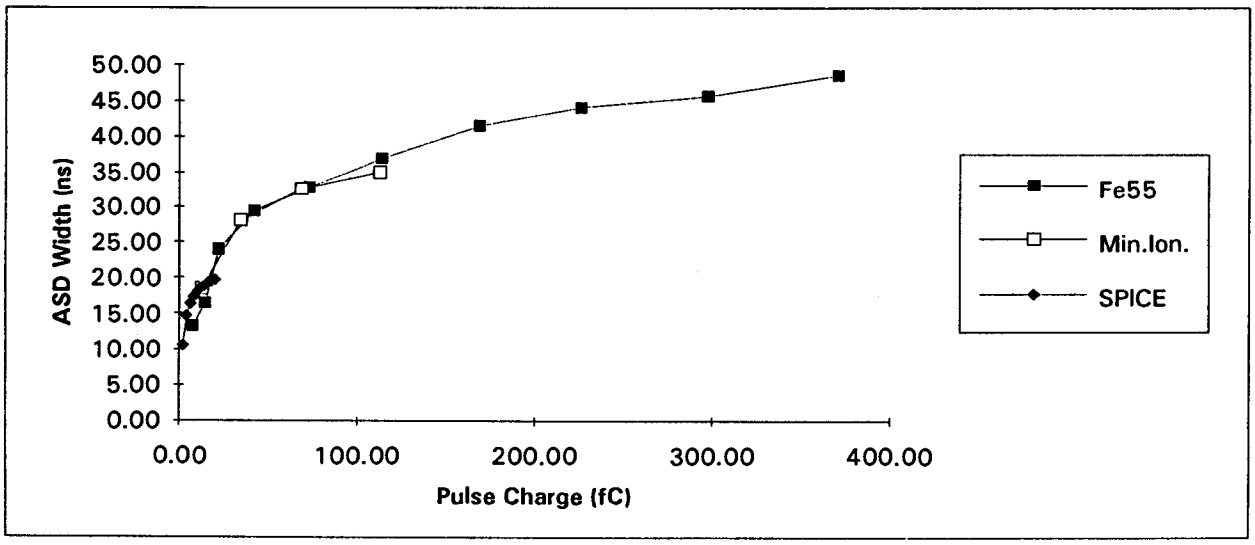
HV	HV/p	Eas*G (10^4)	Qdet (fC)	Fe55	Pulse Width (ns) Min.Ion.	SPICE
1350	1626.51	0.19	7.62	13.30		
1400	1686.75	0.36	14.71	16.40		
1450	1746.99	0.53	22.06	24.00		
1500	1807.23	1.00	42.36	29.30		
1550	1867.47	1.70	73.22	32.80		
1600	1927.71	2.60	113.78	36.90		
1650	1987.95	3.80	168.87	41.50		
1700	2048.19	5.00	225.50	44.00		
1750	2108.43	6.50	297.34	45.60		
1800	2168.67	8.00	371.01	48.50		
1500	1807.23	1.00	12.88		18.40	
1600	1927.71	2.60	34.61		28.00	
1700	2048.19	5.00	68.59		32.50	
1800	2168.67	8.00	112.84		35.00	
			2.00			10.6
			4.00			14.7
			6.00			16.3
			8.00			17.3
			10.00			18
			12.00			18.5
			14.00			18.9
			16.00			19.2
			18.00			19.4
			20.00			19.7